

Ultrahigh-resolution laser spectroscopy of the $S_1 \ ^1B_{2u} \leftarrow S_0 \ ^1A_g$ transition of perylene[☆]

Yasuyuki Kowaka^a, Yoshitake Suganuma^a, Noritaka Ashizawa^a, Naofumi Nakayama^b, Hitoshi Goto^c, Takayoshi Ishimoto^d, Umpei Nagashima^{e,f},
Masaaki Baba^{*,a}

^a*Division of Chemistry, Graduate School of Science, Kyoto University, Sakyo-ku, Kyoto 606-8502, Japan*

^b*Conflex Corporation, 2-15-19 Kami-osaki, Shinagawa-ku, Tokyo 141-0021, Japan*

^c*Department of Knowledge-based Information Engineering, Toyohashi University of Technology, Tempaku-cho, Toyohashi 441-8580, Japan*

^d*INAMORI Frontier Research Center, Kyushu University, Motoooka 744, Nishi-ku, Fukuoka 819-0395, Japan*

^e*Research Institute for Computational Sciences, National Institute of Advanced Industrial Science and Technology, Umezono 1-1-1, Tsukuba, Ibaraki 305-8561, Japan*

^f*Core Research for Evolutional Science and Technology, Japan Science and Technology Agency, 4-1-8 Honcho, Kawaguchi 332-0012, Japan*

Abstract

A rotationally resolved ultrahigh-resolution fluorescence excitation spectrum of the $S_1 \leftarrow S_0$ transition of perylene has been observed using a collimated supersonic jet technique in conjunction with a single-mode UV laser. We assigned 1568 rotational lines of the 0_0^0 band, and accurately determined the rotational constants. The obtained value of inertial defect was positive, accordingly, the perylene molecule is considered to be planar with D_{2h} symmetry. We determined the geometrical structure in the S_0 state by *ab initio* theoretical calculation at the RHF/6-311+G(d,p) level, which yielded rotational constant values approximately identical to those obtained experimentally. Zeeman broadening of each rotational line with the external magnetic field was negligibly small, and the mixing with the triplet state was shown to be very small. This evidence indicates that intersystem crossing (ISC) in

[☆]Presented in part at the 64th International Symposium on Molecular Spectroscopy (Ohio State University, June 2009).

*Corresponding author. FAX: +81 75 753 4065
E-mail address: baba@kuchem.kyoto-u.ac.jp

the S_1 $^1B_{2u}$ state is very slow. The rate of internal conversion (IC) is also inferred to be small because the fluorescence quantum yield is high. The rotational constants of the S_1 $^1B_{2u}$ state were very similar to those of the S_0 1A_g state. The slow internal conversion (IC) at the S_1 zero-vibrational level is attributed to a small structural change upon electronic transition.

Key words: , perylene, rotationally resolved fluorescence excitation spectrum, rotational constants, radiationless transition, *ab initio* theoretical calculation

1. Introduction

Perylene is a typical example of molecules known as polycyclic aromatic hydrocarbons (PAHs), making it a good target for the study of investigating the structure and excited-state dynamics of a large molecule by means of high-resolution spectroscopy. It shows a strong absorption band in the visible region and a high fluorescence quantum yield [1, 2, 3]. Intriguingly, its behaviour is inconsistent with the basic rule that radiationless transition is fast in large molecules because of their high density of coupling levels [4]. It is of great importance to accurately determine the perylene's geometrical structure in the S_0 and S_1 states, because the rate of radiationless transition is strongly dependent on molecular structure. Perylene possesses 20 π electrons which does not conform to Hückel's rule that cyclic planar molecules in which each atom has a p orbital are aromatic and stable if they contain $4n + 2$ π electrons. Phosphorescence was very weak even in cold solid media [5], suggesting that the singlet-triplet mixing by spin-orbit interaction is small and that intersystem crossing (ISC) is very slow in the S_1 state of perylene. Another important process is internal conversion (IC) to the S_0 state by nonadiabatic vibronic interaction. The rate of IC is strongly related to geometrical molecular structure and potential energy curves. We observed the rotationally resolved ultrahigh-resolution spectrum of the $S_1 \leftarrow S_0$ 0_0^0 band of jet-cooled perylene and accurately determined the rotational constants at the zero-vibrational levels of both the S_0 and S_1 states. It is very hard, however, to determine the geometrical structure of a large molecule from its rotational constants alone though not impossible. We therefore performed *ab initio* theoretical calculation to evaluate the structural parameters with reference to the accurately determined rotational constants. In this article, we present the results of ultrahigh-resolution spectroscopy and theoretical

calculation, and discuss their implications for the structure and excited-state dynamics of the isolated perylene molecule.

2. Experimental

Perylene (Wako Chemical) was used as purchased without further purification. The solid sample was kept at 190 °C in a stainless steel container and the vapor was mixed with He gas. The mixed gas was expanded through a pulsed nozzle (an automobile fuel injector) to generate a supersonic jet, which was collimated using a skimmer (2 mm orifice diameter) and a slit (2 mm width). This collimated supersonic jet was crossed with a laser beam at right angles. The distance between the nozzle and the crossing point was 30 cm. The residual Doppler width is estimated to be 0.0001 cm^{-1} under this condition.

As a light source, we employed a cw ring Ti:Sapphire laser (Coherent CR899-29, $\Delta E = 0.0001\text{ cm}^{-1}$) pumped by a Nd:YVO₄ laser (Spectra-Physics, Millennia Xs, 532 nm, 10W). The second harmonics was generated using an enhancement cavity (Spectra-Physics, Wavetrain-SC, LBO), and the power at 401 nm was 10 mW. Fluorescence from excited molecules was collected using a combination of a spherical mirror and an ellipsoidal mirror with a 90% efficient solid angle, and was detected using a photomultiplier (Hamamatsu R585) through a glass filter (Toshiba L42) to block the scattered laser light. The output of the photomultiplier was processed through a gated photon counter (Stanford Research SR400). The change in fluorescence intensity with the laser wavelength was recorded as a fluorescence excitation spectrum. We simultaneously recorded frequency marks and a Doppler-limited absorption spectrum of iodine in order to calibrate transition wavenumbers of rotational lines. A part of the laser output was phase-modulated at 30 MHz by an electro-optic modulator (New Focus 4002), and was passed through a confocal etalon with a focal length of 50 cm (Burleigh, CFT-500, FSR = 150 MHz, finesse = 30). The transmitted light intensity was recorded as frequency marks. The cavity length was stabilized using a cw single-mode green laser (InnoLight, Prometheus 20, 532 nm, 20 mW) with its wavelength tuned to a hyperfine line of iodine. Transition wavenumbers of rotational lines in the Doppler-limited absorption spectrum of iodine were calibrated according to an atlas [6]. The relative and absolute accuracies were 0.0002 and 0.003 cm^{-1} , respectively.

3. Results and Discussion

The molecular structure and coordinate axes of perylene are illustrated in Fig. 1. As shown later, the isolated perylene molecule is considered to be planar with D_{2h} symmetry. Because the three coordinate axes are all equivalent in the D_{2h} symmetry, we must rigorously define the axis notation. Here, we consider the x and y axes the in-plane short and long axes, respectively. The z axis is out-of-plane. The fluorescence excitation spectrum and dispersed fluorescence spectra of the $S_1 \leftrightarrow S_0$ transition of jet-cooled perylene have been already reported [7, 8, 9, 10, 11]. The 0_0^0 band is strongly observed at 401 nm. In addition, we have observed the rotationally resolved ultrahigh-resolution fluorescence excitation spectrum. The whole band is shown in Fig. 2. A sharp peak of the Q branch is clearly seen at the band center, indicating that this transition is an a -type transition, and that the transition moment is parallel to the a axis with the selection rules of $\Delta K_a = 0$, $\Delta K_c = \pm 1$, and $\Delta J = 0, \pm 1$. The S_1 state is therefore identified as ${}^1B_{2u}$. Perylene is a typical asymmetric-top molecule, in which the A , B , and C values are all remarkably different. We analyzed the rotational level energies using the A -reduced Hamiltonian method as presented by Watson [12]. The nonvanishing matrix elements are given by

$$\begin{aligned}
 & \langle JKM | H_r^{(A)} | JKM \rangle \\
 &= \frac{1}{2}(B+C)J(J+1) + \left[A - \frac{1}{2}(B+C) \right] K^2 \\
 & \quad - \Delta_J J^2(J+1)^2 - \Delta_{JK} J(J+1)K^2 - \Delta_K K^4, \tag{1}
 \end{aligned}$$

$$\begin{aligned}
 & \langle JK \pm 2M | H_r^{(A)} | JKM \rangle \\
 &= \left\{ \frac{1}{4}(B-C) - \delta_J J(J+1) - \frac{1}{2}\delta_K [(K \pm 2)^2 + K^2] \right\} \\
 & \quad \times \{ [J(J+1) - K(K \pm 1)][J(J+1) - (K \pm 1)(K \pm 2)] \}^{1/2}, \tag{2}
 \end{aligned}$$

where $|JKM\rangle$ is the eigenfunction of a symmetric-top molecule. J is a quantum number of the total angular momentum \mathbf{J} , and K and M are quantum numbers of the projections of \mathbf{J} along the molecule-fixed z axis and the space-fixed Z axis, respectively. The matrix elements are independent of M in the absence of the magnetic field. A , B , and C are the rigid

rotor rotational constants. Δ_J, Δ_{JK} , and Δ_K are the symmetric-top quartic centrifugal distortion constants, and δ_J and δ_K are the asymmetric-top distortion constants.

We iterated a procedure of assigning rotational lines and improving rotational constants, and finally obtained accurate rotational constants by a least-squares fit of 1568 assigned lines. The resultant values are listed in Table 1. The spectrum calculated using these constants and assuming a rotational temperature of 7 K was in good agreement with the observed spectrum. The observed and calculated spectra near the band origin are shown in Fig. 3. Strong transitions from low K_a'' levels overlap within the natural linewidth and give rise to prominent regular peaks. We achieved the best agreement assuming a linewidth of 0.001 cm^{-1} , corresponds to a fluorescence lifetime of 5.3 ns. This is appreciably shorter than the observed lifetime by real-time measurement (8.88 ns) [9]. The discrepancy may be attributed to saturation broadening in the ultrahigh-resolution spectrum because this transition is very strong. Fig. 4 shows the similar spectra in the lower wavenumber region. The prominent lines are assigned as ${}^qP_{K_a''=0,1}(J'')$. The spectrum calculated using these constants is also in good agreement with the observed spectrum.

The value of inertial defect $\Delta = I_c - I_b - I_a$ was calculated to be $2.0085 \text{ amu}\text{\AA}^2$ based on the determined rigid rotor rotational constants. The inertial defect of a hypothetical rigid or frozen molecule is represented by

$$\Delta = -2 \sum_i m_i c_i^2 \quad (3)$$

where m_i and c_i are the mass and the out-of-plane (z) coordinate of the i th atom, respectively. Therefore, the inertial defect is vanishing for a planar frozen molecule and the Δ value is assumed to be zero. If the molecule is nonplanar, the Δ value must be negative. The experimental value is, however, slightly different from the expected value, because of vibration-rotation interaction or average on zero-point vibration [13, 14]. In a large planar aromatic molecule, the zero-point inertial defect is small and negative, and is empirically expressed as [15]

$$\Delta_0 = -\frac{3.715}{\nu_1} + 0.00803\sqrt{I_c}, \quad (4)$$

where I_c and Δ_0 are in units of $\text{amu}\text{\AA}^2$. ν_1 is the lowest energy of out-of-plane vibration in units of cm^{-1} . The first negative term arises from an out-of-plane

vibration of the lowest frequency mode. The second positive term expresses the effect of in-plane zero-point vibration. In fact, the values of inertial defect are small and negative for large PAH molecules such as naphthalene ($-0.15 \text{ amu}\text{\AA}^2$) [16, 17], anthracene ($-1.08 \text{ amu}\text{\AA}^2$) [18] and pyrene ($-0.65 \text{ amu}\text{\AA}^2$) [19]. In perylene, the second positive term is estimated to be $0.39 \text{ amu}\text{\AA}^2$. The experimental value ($2.0085 \text{ amu}\text{\AA}^2$), however, is much larger than this. At the very least, we can conclude that the perylene molecule is planar, and that its symmetry is identified to be D_{2h} , because the second positive term would have to be negative for a nonplanar molecule. The positive inertial defects were found in many small planar molecules [20]. The large positive value in perylene may be due to large contribution of symmetric in-plane vibrations. The perylene molecule actually possesses a large number of symmetric in-plane modes and the energies of some of them are small.

Perylene has 20 π electrons and does not conform to Hückel’s rule in the same manner as pyrene [19], the equilibrium structure of which is the symmetrized form of two mesomeric structures of localized double bonds. In order to confirm this and to estimate the geometrical structure, we carried out *ab initio* theoretical calculation using the Gaussian 03 program package [21]. First, we calculated the rotational constants of the S_0 state with the geometrical optimization of several calculational methods retaining D_{2h} symmetry. The restricted Hartree-Fock (RHF) method with a 6-311+G(d,p) basis set yielded $A = 0.0211130$, $B = 0.0111056$, and $C = 0.00727753 \text{ cm}^{-1}$, all of which are astonishingly close to the experimentally obtained values of $A = 0.0211320$, $B = 0.0111077$, and $C = 0.0072744 \text{ cm}^{-1}$. The errors are 0.09, 0.02 and 0.04% for the A , B , and C values, respectively. Consequently, we consider the geometrical structure that we calculated to be accurate for the isolated perylene molecule in the S_0 state. The resultant bond lengths and bond angles are shown in Fig. 5. We calculated the rotational constants with various bond lengths and could estimate the accuracy of these calculations to be $2 \text{ m}\text{\AA}^2$ for the C-H bond and $0.2 \text{ m}\text{\AA}^2$ for the C-C bond. Although the RHF method does not sufficiently account for electronic correlation, the rotational constants calculated using this method are almost identical to the experimentally obtained ones. The error in the A value is slightly large, but they can probably be attributed to the effect of zero-point vibration, which can not be incorporated into *ab initio* calculation. We also performed RCIS calculation for the S_1 state, but the resultant values for rotational constants and excitation energy were not sufficiently similar to the experimental values. In future studies, we intend to perform calculations at a higher level

such as SAC-CI, as this method has been shown to be very powerful in the anthracene molecule [18].

The transition wavenumbers of observed lines were all in good coincidence with calculated transition wavenumbers using the obtained rotational constants. We found no energy shift occurring as a result of local perturbation; accordingly, the mixing with the triplet state is considered to be small. We have already identified many level shifts and large Zeeman broadening in the S_1 ($n\pi^*$) states of glyoxal [22] and pyrazine [23], in which the singlet-triplet coupling through spin-orbit interaction is strong. We have now observed the ultrahigh-resolution spectrum of perylene in the external magnetic field of 1 Tesla. However, we could find no change in the spectrum, and the Zeeman broadening of M_J levels has been shown to be fairly small. This indicates that singlet-triplet interaction is very weak and that ISC is minor in the S_1 ${}^1B_{2u}$ ($\pi\pi^*$) state of perylene. This is common among other PAH molecules such as naphthalene [16, 17], anthracene [18], and pyrene [19], and is consistent with El-Sayed's rule that spin-orbit interaction between the ${}^1\pi\pi^*$ and ${}^3\pi\pi^*$ states is very weak for a planar molecules with π bonds [24]. The El-Sayed's rule also states that mixing between the ${}^1n\pi^*$ and ${}^3\pi\pi^*$ states is large, which is true in the cases of glyoxal and pyrazine.

Another possible radiationless process in the S_1 state is IC, which is caused by vibronic interaction with high-vibrational levels of the S_0 state. The IC rate is given by [4, 25, 26, 27]

$$\begin{aligned}
W_{IC} &\propto \sum_i \left| \left\langle \phi_{S_0} \left| \frac{\partial}{\partial Q_i} \right| \phi_{S_1} \right\rangle \right|^2 \left| \left\langle \chi_{S_0}^{v''} \left| \frac{\partial}{\partial Q_i} \right| \chi_{S_1}^{v'=0} \right\rangle \right|^2 \delta(E_{S_1}^{v'=0} - E_{S_0}^{v''}) \\
&\approx \frac{\sum_i \left| \left\langle \phi_{S_0}(r, Q_0) \left| \left(\frac{\partial U(r, Q)}{\partial Q_i} \right)_{Q_0} \right| \phi_{S_1}(r, Q_0) \right\rangle \right|^2}{(E_{S_1}(Q_0) - E_{S_0}(Q_0))} \\
&\quad \times \left| \left\langle \chi_{S_0}^{v''}(Q_i) \left| \frac{\partial}{\partial Q_i} \right| \chi_{S_1}^{v'=0}(Q_i) \right\rangle \prod_{j \neq i} \left\langle \chi_{S_0}^{v''}(Q_j) \left| \chi_{S_1}^{v'=0}(Q_j) \right\rangle \right|^2 \\
&\quad \times \delta(E_{S_1}^{v'=0} - E_{S_0}^{v''}) . \tag{5}
\end{aligned}$$

ϕ_{S_0} and ϕ_{S_1} are the electronic wavefunctions of the S_0 and S_1 states, respectively. $\chi_{S_0}^{v''}$ is the vibrational wavefunction of the high-vibrational level in the S_0 state, and $\chi_{S_1}^{v'=0}$ is that of the zero-vibrational level in the S_1 state. δ is the

Dirac delta function. Q_i is a normal coordinate and Q_0 represents the equilibrium position. The second matrix element is non-adiabatic Franck-Condon overlap of a promoting mode and the third is Franck-Condon overlap of other modes. The S_1 ${}^1B_{2u}$ and S_0 1A_g states are coupled by a b_{2u} vibration. The IC rate is zero when the equilibrium molecular structure and potential energy curves are identical for the S_0 and S_1 states. In large PAH molecules, the π orbital is uniformly distributed over the whole molecule. The bond orders and energies are not significantly changed by electronic excitation, and the small changes are further diluted with a large number of π electrons. Therefore, the structural change arising from the $\pi\pi^*$ excitation is generally expected to be small. This similarity in the molecular structures of the S_0 and S_1 states has been demonstrated in pyrene [19]. The obtained rotational constants of the S_1 ${}^1B_{2u}$ state of perylene are also very similar to those of the S_0 1A_g state. This small structural change can be understood through an examination of the π orbitals shown in Fig. 6, which were calculated at the RHF/STO-3G level. The S_1 ${}^1B_{2u}$ state is principally represented by the configuration of HOMO – LUMO one-electron excitation. The wavefunctions are uniformly distributed over the whole molecule in HOMO and LUMO. Consequently, the bond orders and the slopes of potential energy curves are also expected to be similar between the S_0 and S_1 states. Therefore, the small IC rate can be attributed to the small scale of the structural change that occurs upon electronic excitation.

In conclusion, we observed the rotationally resolved ultrahigh-resolution spectrum of the S_1 ${}^1B_{2u} \leftarrow S_0$ 1A_g 0_0^0 band of jet-cooled perylene and determined the rotational constants at the zero-vibrational levels of the S_0 and S_1 states. Because the value of inertial defect is positive, the isolated perylene molecule is considered to be planar. *Ab initio* theoretical calculation at the RHF/6-311+G(d,p) level yielded the rotational constants of the S_0 state approximately equal to the experimentally obtained ones. We consider our calculated geometrical structure to be an accurate representation of the structure of the isolated perylene molecule. It is worth noting that the rotational constants of the S_1 state are very similar to those of the S_0 state. This indicates that the structural change that occurs upon electronic excitation is very small. The slow IC process can be attributed to the small scale of this structural change.

Acknowledgements

This research was supported by Grant-in-Aid for the Global COE Program, "International Center for Integrated Research and Advanced Education in Materials Science", from the Ministry of Education, Culture, Sports, Science and Technology of Japan. We are grateful to M. Aoyama, M. Kondo, T. Yano, N. Mizutani, and M. Suzui (Equipment Development Center, Institute for Molecular Science), and K. Mitsui, and N. Okada (Advanced Technology Center, National Astronomical Observatory Japan) for their help in making a mirror set for high-efficiency fluorescence collection. The authors thank Professor S. Kasahara (Molecular Photoscience Research Center, Kobe University, Japan) for his kind help. M. B. thanks Professor Takeshi Oka (The University of Chicago) for his helpful advice and suggestions.

References

- [1] M. Lamotte, A.M. Merle, J. Joussot-Dubien, F. Dupuy, *Chem. Phys. Lett.* 35 (1975) 410-416.
- [2] I.I. Abram, R.A. Auerbach, R.R. Birge, B.E. Kohler, J.M. Stevenson, *J. Chem. Phys.* 63 (1975) 2473-2478.
- [3] J. Olmsted, III, *J. Phys. Chem.* 83 (1979) 2581-2584.
- [4] M. Bixon, J. Jortner, *J. Chem. Phys.* 48 (1968) 715-726.
- [5] J.J. Dekkers, G.Ph. Hoornweg, K.J. Terpstra, C. Maclean, N.H. Velthorst, *Chem. Phys.* 34 (1978) 253-260.
- [6] S. Gerstenkorn, P. Luc, *Atlas du Spectre d'Absorption de la Molecule D'Iode*, CNRS, Paris, 1978.
- [7] B.E. Forch, K.T. Chen, E.C. Lim, *Chem. Phys. Lett.* 100 (1983) 389-392.
- [8] S.A. Schwartz, M.R. Topp, *Chem. Phys.* 86 (1984) 245-255.
- [9] A.J. Kaziska, S.A. Wittmeyer, A.L. Motyka, M.R. Topp, *Chem. Phys. Lett.* 154 (1989) 199-206.
- [10] M. Sonnenschein, A. Amirav, J. Jortner, *J. Phys. Chem.* 88 (1984) 4214-4218.

- [11] X. Tan, F. Salama, *J. Chem. Phys.* 122 (2005) 084318/1-9.
- [12] J.K.G. Watson, *Vibrational Spectra and Structure*, in J.R. Durig (Ed.), Elsevier, New York, 1977, pp. 1-89.
- [13] D.R. Herschbach, V.W. Laurie, *J. Chem. Phys.* 40 (1964) 3142-3153.
- [14] T. Oka, Y. Morino, *J. Mol. Spectrosc.* 6 (1961) 472-482.
- [15] T. Oka, *J. Mol. Struct.* 352/353 (1995) 225-233.
- [16] M. Okubo, J. Wang, M. Baba, M. Misono, S. Kasahara, H. Katô, *J. Chem. Phys.* 122 (2005) 144303/1-7.
- [17] K. Yoshida, Y. Semba, S. Kasahara, T. Yamanaka, M. Baba, *J. Chem. Phys.* 130 (2009) 194304/1-6.
- [18] M. Baba, M. Saitoh, K. Taguma, K. Shinohara, K. Yoshida, Y. Semba, S. Kasahara, N. Nakayama, H. Goto, T. Ishimoto, U. Nagashima, *J. Chem. Phys.* 130 (2009) 134315/1-9.
- [19] M. Baba, M. Saitoh, Y. Kowaka, K. Taguma, K. Yoshida, Y. Semba, S. Kasahara, Y. Ohshima, T. Yamanaka, Y.-C. Hsu, S.H. Lin, *J. Chem. Phys.* 131 (2009) in press.
- [20] W. Gordy, R.L. Cook, in W. West (Ed.), *Microwave Molecular Spectra*, John Wiley & Sons, New York, 1970, pp. 528.
- [21] M.J. Frisch, G.W. Trucks, H.B. Schlegel, G.E. Scuseria, M.A. Robb, J.R. Cheseman, J.A. Montgomery, Jr., T. Vreven, K.N. Kudin, J.C. Burant, J.M. Millam, S.S. Iyengar, J. Tomasi, V. Barone, B. Mennucci, M. Cossi, G. Scalmani, N. Rega, G.A. Petersson, H. Nakatsuji, M. Hada, M. Ehara, K. Toyota, R. Fukuda, J. Hasegawa, M. Ishida, T. Nakajima, Y. Honda, O. Kitao, H. Nakai, M. Klene, X. Li, J.E. Knox, H.P. Hratchian, J.B. Cross, C. Adamo, J. Jaramillo, R. Gomperts, R.E. Stratmann, O. Yazyev, A.J. Austin, R. Cammi, C. Pomelli, J.W. Ochtersky, P.Y. Ayala, K. Morokuma, G.A. Voth, P. Salvador, J.J. Dannenberg, V.G. Zakrzewski, S. Dapprich, A.D. Daniels, M.C. Strain, O. Farkas, D.K. Malick, A.D. Rabuck, K. Raghavachari, J.B. Foresman, J.V. Ortiz, Q. Cui, A.G. Baboul, S. Clifford, J. Cioslowski, B.B. Stefanov, G. Liu, A. Liashenko, P. Piskorz, I. Komaromi, R.L. Martin, D.J. Fox, T.

Keith, M.A. Al-Laham, C.Y. Peng, A. Nanayakkara, M. Challacombe, P.M.W. Gill, B. Johnson, W. Chen, M.W. Wong, C. Gonzalez, J.A. Pople, *Gaussian 03*, revision B.05, Gaussian, Inc., Pittsburgh PA, 2003.

- [22] H. Katô, K. Sawa, H. Kuwano, S. Kasahara, M. Baba, S. Nagakura, J. Chem. Phys. 109 (1998) 4798 - 4806.
- [23] N. Yamamoto, T. Ebi, M. Baba, J. Chem. Phys. 105 (1996) 5745-5752.
- [24] M.A. El-Sayed, J. Chem. Phys. 38 (1963) 2834-2838.
- [25] S.H. Lin, J. Chem. Phys. 44 (1966) 3759-3767.
- [26] C.H. Chin, H.Y.-J. Shiu, H.-W. Wang, Y.-L. Chen, C.-C. Wang, S.H. Lin, M. Hayashi, J. Chin. Chem. Soc. 53 (2006) 131-152.
- [27] W. Siebrand, J. Chem. Phys. 46 (1967) 440-447.

Table 1

Molecular constants of the $S_0 \ ^1A_g(v'' = 0)$ and $S_1 \ ^1B_{2u}(v' = 0)$ states. The rotational constants A , B , C , Δ_J , Δ_{JK} , Δ_K , δ_J , δ_K , band origin ν_0 , and standard deviation σ are in units of cm^{-1} . The Moments of inertia I_a , I_b , I_c and inertial defect Δ are in units of $\text{amu}\text{\AA}^2$.

Perylene	$S_0 \ ^1A_g(v'' = 0)$	$S_1 \ ^1B_{2u}(v' = 0)$
A	0.021132(45)	0.020847(45)
B	0.0111077(60)	0.0112638(58)
C	0.0072744(39)	0.0073044(38)
$D_K(\times 10^{-7})$	-2.6(21)	-2.6(21)
$D_{JK}(\times 10^{-8})$	3.8(17)	3.6(17)
$D_J(\times 10^{-9})$	-6.4(25)	-6.6(24)
$\delta_K(\times 10^{-8})$	-9.0(22)	-9.0(20)
$\delta_J(\times 10^{-9})$	-3.5(14)	-3.6(13)
κ	-0.4468	-0.4153
I_a	797.73	808.64
I_b	1517.65	1496.62
I_c	2317.39	2307.87
Δ	2.0085	2.6174
T_0	-	24059.372(3)
σ	-	0.00040
fit lines	-	1568
band type		a

Figure Captions

Fig. 1 Molecular structure, and coordinate and rotational axes of perylene.

Fig. 2 Ultrahigh-resolution fluorescence excitation spectra of the 0_0^0 band of the $S_1 \leftarrow S_0$ transition of perylene in a collimated supersonic jet.

Fig. 3 The observed (Obs.) and calculated (Calc.) ultrahigh-resolution fluorescence excitation spectra of the 0_0^0 band near the band center. Assignments are indicated by the lines above the observed spectrum.

Fig. 4 The observed (Obs.) and calculated (Calc.) ultrahigh-resolution fluorescence excitation spectra of the 0_0^0 band in the lower wavenumber region. Assignments are indicated by the lines above the observed spectrum.

Fig. 5 Molecular structure of perylene in the S_0 state as determined by *ab initio* theoretical calculation at the RHF/6-311+G(d,p) level. Bond lengths are in units of Å.

Fig. 6 π orbitals of perylene calculated at the RHF/STO-3G level.

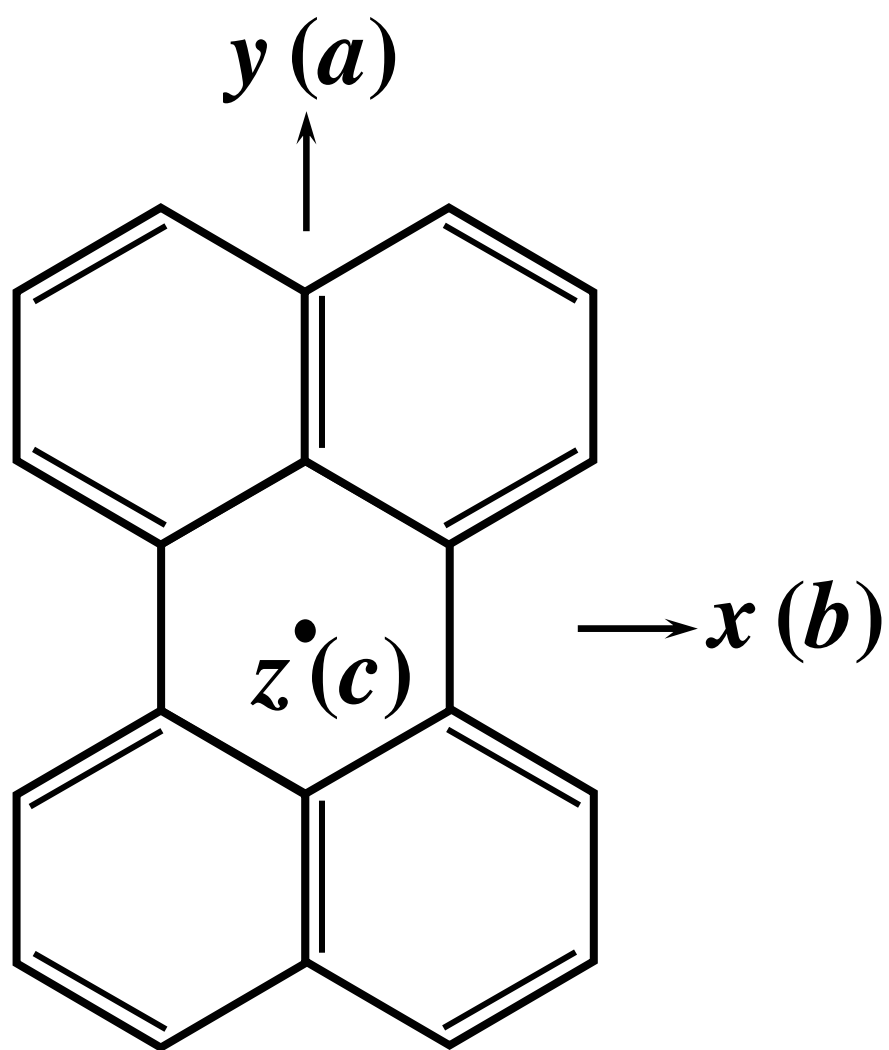


Fig. 1. Y. Kowaka *et al.*

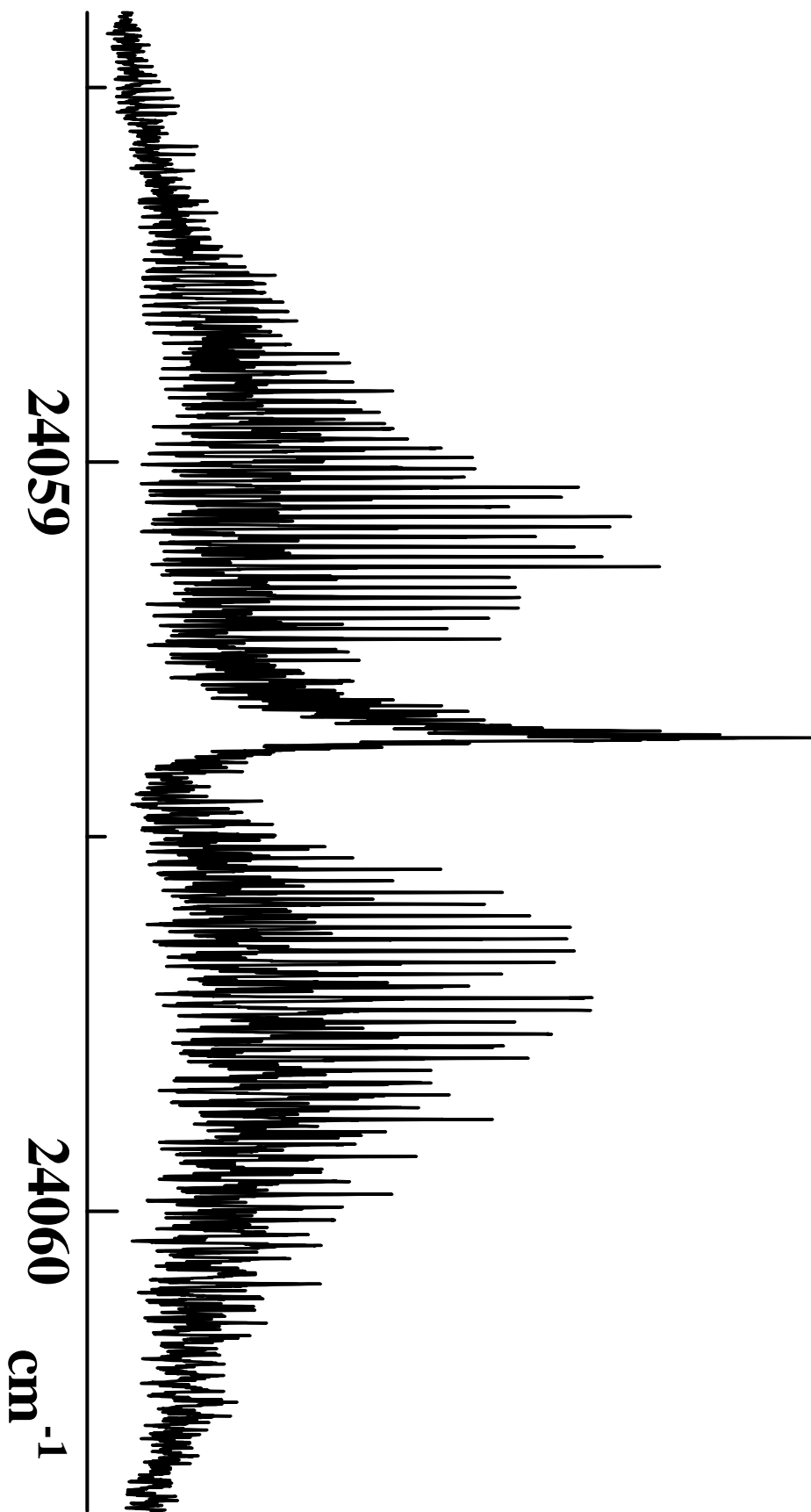


Fig. 2. Y. Kowaka *et al.*

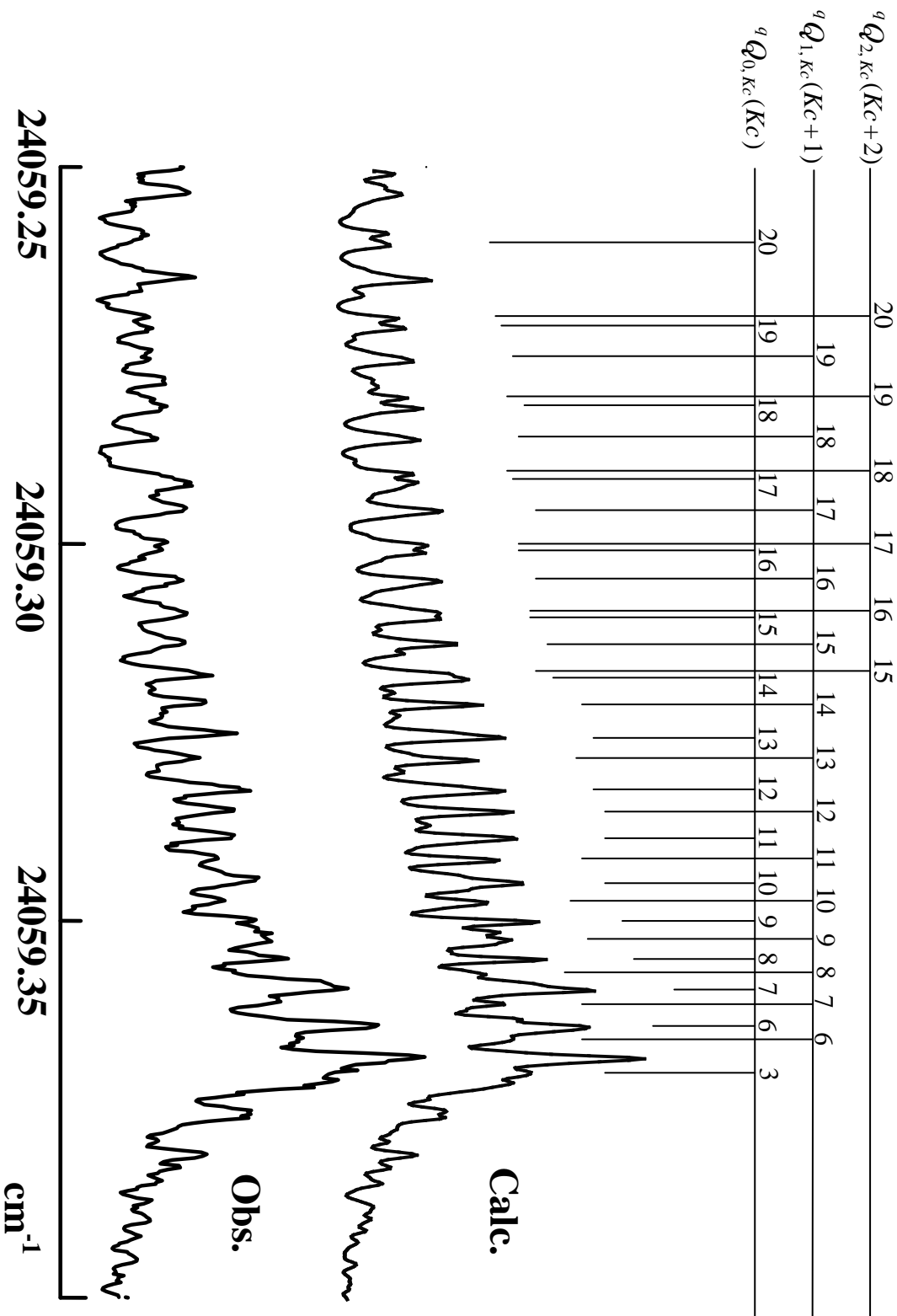


Fig. 3. Y. Kowaka *et al.*

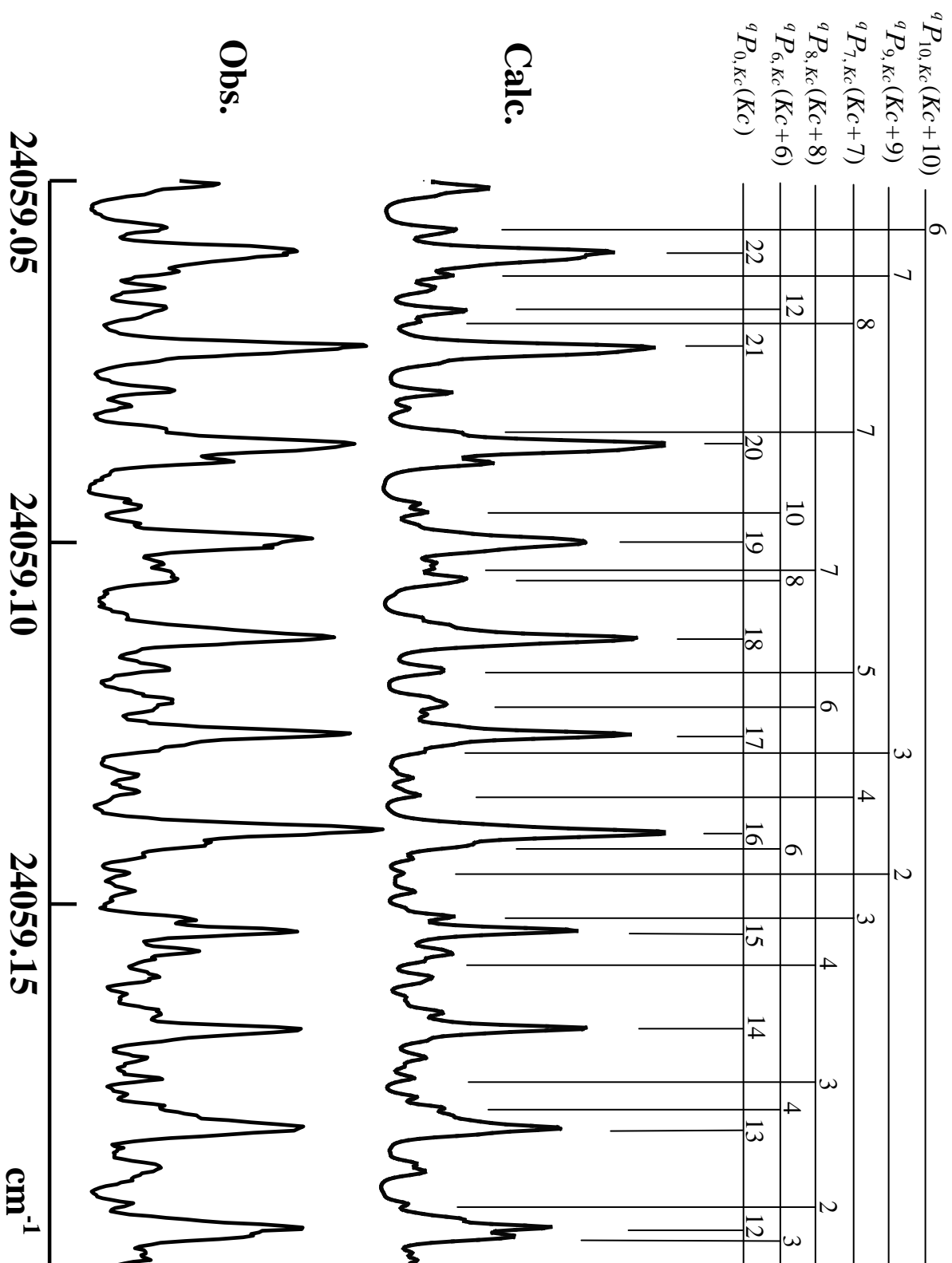


Fig. 4. Y. Kowaka *et al.*

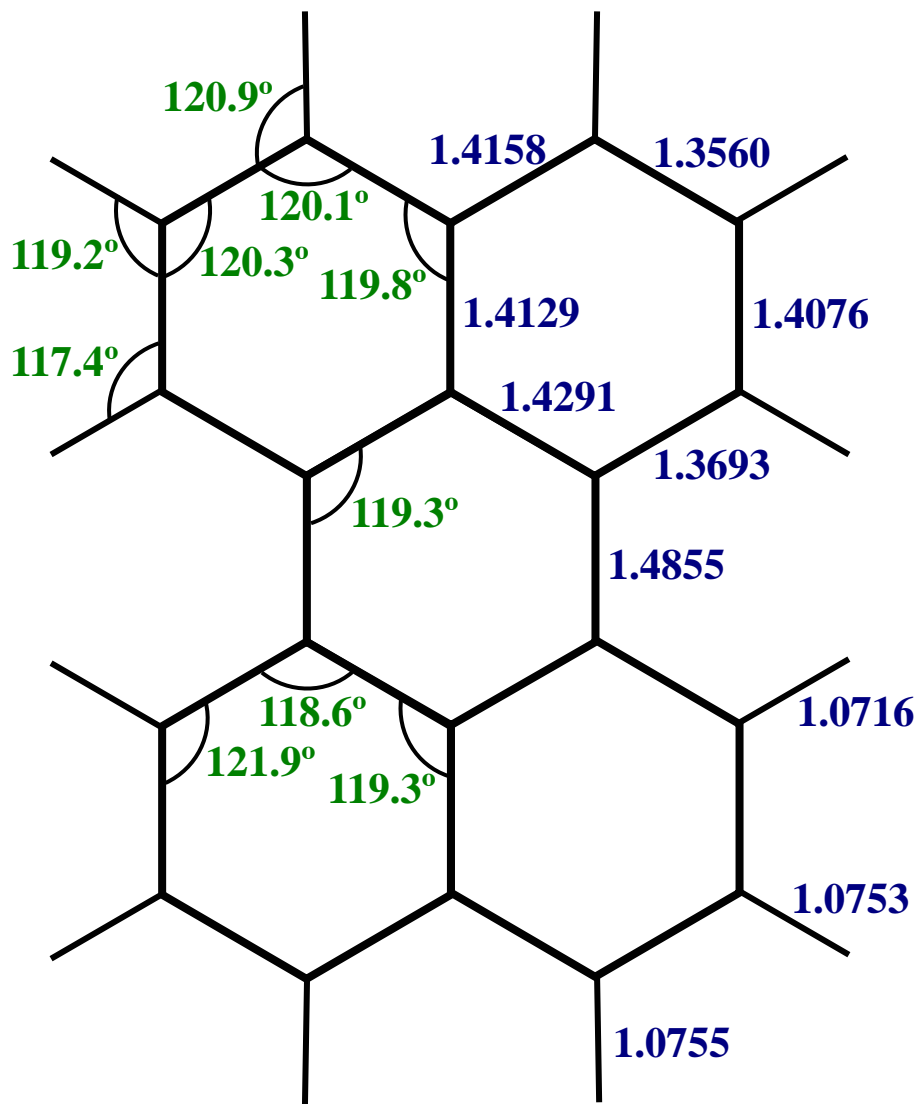


Fig. 5. Y. Kowaka *et al.*

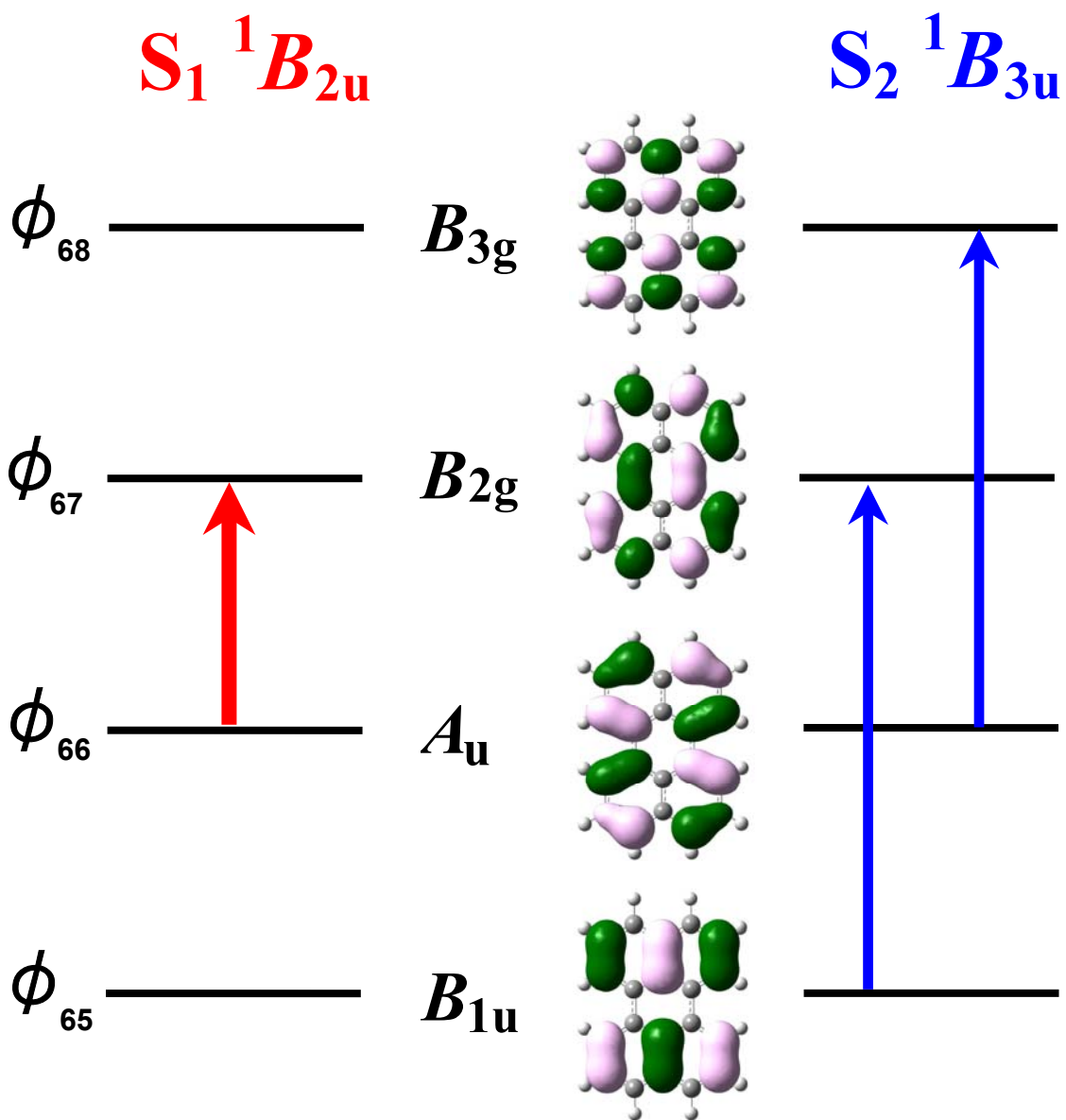


Fig. 6. Y. Kowaka *et al.*